Ultrasonographic identification of fibromuscular bands associated with neurogenic thoracic outlet syndrome: the 'wedge-sickle' sign

Zsuzsanna Arányi MD, PhD[1], Anita Csillik MD[1], Josef Böhm MD, PhD[2], Thomas Schelle MD[3]

[1]MTA-SE NAP B Peripheral Nervous System Research Group, Dept. of Neurology, Semmelweis University, Balassa u. 6, 1083 Budapest, Hungary

[2]Neurologische Praxis, Dr. Friedrich Behse/Dr. Josef Böhm, Kurfürstendamm 69, 10707 Berlin, Germany

[3]Dept. of Neurology, Städtisches Klinikum Dessau, Auenweg 38, 06847 Dessau-Roßlau, Germany

Corresponding author:

Zsuzsanna Arányi MD, PhD

Dept. of Neurology, Semmelweis University

Address: Balassa u. 6, Budapest, Hungary-1083

E-mail: aranyi.zsuzsanna@med.semmelweis-univ.hu

Tel.: +36-20-825-0357, Fax: +36-1-210-1368

ABSTRACT

Thoracic outlet syndrome (TOS) is a disorder characterized by the compression of the lower trunk of the brachial plexus most often in association with anomalous congenital fibromuscular bands in the scalenic region. Early diagnosis is important, because the neurological deficit associated with TOS may be irreversible. Using high resolution ultrasound, we investigated 20 consecutive patients with clinical signs suggestive of TOS (all females, average age: 40.4 ± 14.9 years), and 25 control subjects. In 19 patients, a hyperechoic fibromuscular structure at the medial edge of the middle scalene muscle was identified, which indented the lower trunk of the brachial plexus (‘*wedge-sickle sign’*). It was associated with the significant enlargement ($P<0.0001$) and hypoechogenicity of the lower trunk. This novel and distinctive ultrasonographic sign allows the presurgical identification of anomalous fibromuscular bands causing TOS. It is especially useful in patients without neurological deficit, where the diagnosis may not be as straightforward.

Key words: thoracic outlet syndrome, high resolution ultrasound, fibromuscular bands, wedge-sickle sign

INTRODUCTION

The term thoracic outlet syndrome (TOS) was coined for a group of disorders characterized by the compression of the brachial plexus or the subclavian vessels at any point in the thoracic outlet region (Peete et al. 1956). According to the classification presently in use, it comprises five distinct clinical syndromes: arterial vascular TOS, venous vascular TOS, traumatic neurovascular TOS, true neurologic (neurogenic) TOS, and nonspecific TOS (Wilbourn 1999; Ferrante 2012). In neurogenic TOS, the brachial plexus is typically compressed in the scalenic triangle at the level of the lower trunk or the distal portion of its constituents, the C8 and Th1 anterior primary rami ('roots'). This gives rise to a characteristic clinical syndrome with the selective wasting of the thenar and the first dorsal interosseous muscle (Gilliatt et al. 1970), and sensory disturbance on the medial aspect of the forearm, with or without pain in the affected arm. The electrophysiological hallmark of neurogenic TOS is the demonstration of postganglionic sensorimotor C8-Th1 axon loss, with Th1 being affected more and earlier (Tsao et al. 2014). The category 'nonspecific TOS', also called 'disputed TOS' (Wilbourn 1999), is a controversial category with a lack of consensus on its aetiology, pathomechanism and treatment. It is characterized by subjective symptoms such as pain and paraesthesia in the arm, and the feeling of fatigue of the arm, especially when lifted overhead, with no clinical deficit.

Congenital anomalies or anatomic variations of the thoracic outlet region, particularly the supernumerary cervical rib attached to the 7^{th} cervical vertebra, have been historically implicated in TOS (Roos 1976). However, given that the estimated prevalence of cervical ribs in the general population is 0.5-2% (Ferrante 2012; Viertel et al. 2012) and that of neurogenic TOS is 1 per million (Gilliatt et al. 1970), statistically the presence of a cervical rib is in itself not diagnostic for neurogenic TOS (Ferrante 2012; Weber and Criado 2014). Its relevance appears to be higher for arterial vascular TOS (Weber and Criado 2014). Roos, with an extensive surgical experience in TOS, was the first to focus attention on anomalous fibromuscular bands with or without a cervical rib in the thoracic outlet region as the real culprit for neurogenic TOS (Roos 1976; Roos 1980; Brantigan and Roos 2004). He described 10 types of these bands affecting the lower trunk and 7 affecting the upper or the middle trunks of the brachial plexus (Roos 1976; Brantigan and Roos 2004). These 'Roos ligaments' were

originally identified based on surgical and cadaveric studies, but nowadays modern imaging techniques such as magnetic resonance imaging (MRI) and high resolution ultrasound (HRUS) are available for their possible presurgical detection and the facilitation of diagnosis. Some MRI data are already available (Aralasmak et al. 2012; Luigetti et al. 2012; Matur et al. 2013; Yildizgören et al. 2014; Singh et al. 2014; Baumer et al. 2014; Magill et al. 2015; Poretti et al. 2015). However, literature data regarding ultrasound is limited to a single case report (Simon et al. 2013), despite the ease and accessibility, and the recent advent of HRUS in the diagnosis of peripheral nerve disorders (Hobson-Webb et al. 2012). We present here a consecutive case series of patients with neurogenic and non-specific TOS assessed by HRUS.

PATIENTS AND METHODS

An approval for the retrospective analysis of patient data was obtained from both Institutional Ethics Committees. Twenty consecutive patients, assessed at two tertiary referral centres for neuromuscular disorders between 2014 and 2016, were included in the analysis (*Table 1*). Inclusion criteria of patients in the study were the clinical symptoms and signs suggestive of TOS and the exclusion of other disorders, such as carpal tunnel syndrome, ulnar nerve lesion, and C8-Th1 radiculopathy. All patients gave informed consent to the examinations, and retrospective analysis was performed using anonymized patient data. Healthy controls were examined prospectively with informed consent.

All patients underwent clinical, electrophysiological, and ultrasound assessments, and radiographic examination of the cervical spine to look for a cervical rib or elongated transverse process of the 7^{th} cervical vertebra. Additional examinations (e.g. MRI of the cervical spine) were also carried out if deemed necessary for differential diagnosis. ‘Neurogenic TOS’ was diagnosed if unequivocal clinical *and* electrophysiological signs of postganglionic sensorimotor C8-Th1 axon loss were demonstrated, unexplained by any other cause. ‘Non-specific TOS’ was diagnosed when subjective complaints suggesting TOS were present without neurological deficit (clinical signs of C8-Th1 lesion), with or without electrophysiological alterations typical for TOS. Subjective complaints

suggesting TOS included pain and paraesthesia in the arm, especially when lifted overhead, the feeling of fatigability of the arm, and Tinel sign at the supraclavicular fossa. The paraesthesia typically involves the medial side of the forearm and hand, but some patients may not be able to localize it and complain of paraesthesia of the whole arm. Provocative manoeuvres, such as the Roos-test (elevated arm stress test), were not used as a diagnostic element, as they were deemed unreliable (Plewa and Delinger, 1998).

Eight patients underwent surgery for TOS.

Electrophysiology

For the demonstration of postganglionic sensorimotor C8-Th1 axon loss, all patients underwent motor and sensory nerve conduction studies and F waves of the median and ulnar nerves, and nerve conduction study of the medial antebrachii cutaneous nerve (MABC), all with side comparison. Additional examinations, such as needle electromyography of C8-Th1 innervated small hand and forearm muscles were carried out on individual basis. A Viking EMG device manufactured by CareFusion (San Diego, CA, USA) was used for electrophysiological examination.

Ultrasonography

The scanning was performed by three of the authors, Z.A., J. B. and T. S., all of whom are neurologists and clinical neurophysiologists, and have 4, 10 and 8 years of experience, respectively, in nerve sonography. A Philips HD15 XE Pure Wave device with a 12-5 MHz 50 mm linear array transducer and a Philips Epiq 5 device with a 18-5 MHz linear array transducer, manufactured by Philips (Amsterdam, The Netherlands), and a Siemens Acuson Antaris 5.0 device with a 13 MHz linear array transducer, manufactured by Siemens (Munich. Germany) were used. Settings were optimized for nerve imaging, including the use of compound imaging mode. In all patients, the whole supraclavicular portion of the brachial plexus was scanned, according to standard methods and landmarks (Martinoli et al. 2002; Gruber et al. 2007). Axial scanning was started at the supraclavicular fossa, where the lower trunk of the brachial plexus was identified adjacent to the subclavian artery. Scanning was continued cranially up to the C5 root level. Colour Doppler was used to identify blood vessels in the region. Special attention was paid to the lower trunk of the brachial plexus, and any

structures in its vicinity. The cross-sectional area (CSA) of the lower trunk was measured by outlining its outer border, using the continuous trace function of the ultrasound device, at the site of abnormality. More proximally (cranially) the lower trunk breaks up into its constituents, the C8 and the Th1 nerve roots, which were not measured due to their deep position and unreliable identification. The shape of the lower trunk was examined and noted whether it deviated from the normal round shape. Its echogenicity-fascicular structure was also visually assessed as compared to the other elements of the brachial plexus (i.e. upper and middle trunks) in the same patient. No quantification of echogenicity was performed. Sonographic Tinel sign was tested by pressing with the transducer on the region of abnormality. The unaffected side was also examined to check for the presence of any abnormality and sonographic Tinel sign, but CSA measurements were not made.

A control group was also examined to obtain normal values for the CSA of the lower trunk and to check for the occurrence of any abnormality and sonographic Tinel sign in the supraclavicular region. None of the subjects had subjective or objective symptoms and signs suggestive of TOS. Control subjects did not undergo electrophysiological assessment. In all subjects, the measurement was performed on the right side.

Statistics

Descriptive statistics (mean, standard deviation, and range) were applied to describe the age of patients and control subjects, the age of onset of TOS symptoms in patients, and the CSA values of the lower trunk in the affected arms of patients and in control subjects. Two-tailed unpaired t-test was used to test the difference between the age and the CSA values of the control and patient groups. Two-tailed Fisher's exact test was used to test for association between the clinical symptoms and signs suggestive of TOS (including both neurogenic and non-specific TOS) and the presence of the wedge-sickle sign, and between the sonographic Tinel sign and the presence of the wedge-sickle sign. With respect to the clinical symptoms suggestive of TOS, the sensitivity and the positive predictive value of the presence of the wedge-sickle sign and the sonographic Tinel sign were also calculated. For the tests evaluating the wedge-sickle sign and the sonographic Tinel sign, the control group and the

unaffected arms of the patient group were pooled. Statistical significance was set at $p<0.05$. GraphPad software (GraphPad Software, San Diego, CA, USA) was used for statistical calculation.

RESULTS

The patient group included 20 females with a mean age of 40.4 ± 14.9 years (range: 19-74 years). The control group included 25 females with a mean age of 38.9 ± 9.8 years (range: 17-51 years). No significant difference was found between the age of the two groups ($p=0.6917$). Thus, the composition of the patient and the control groups with respect to age and sex was homogeneous. *Table 1* shows the summary of demographic, clinical, electrophysiological and radiographic data for all patients, including the individual CSA measurements of the lower trunk. The mean age at the onset of symptoms in the patient group was 34.9 ± 13.5 years (range: 14-69 years). All patients were right-handed and all patients had unilateral symptoms. In 17 patients, symptoms were on the right side. Fifteen patients were diagnosed with 'neurogenic TOS', with clinical and electrophysiological signs of postganglionic sensorimotor C8-Th1 axon loss. C8 involvement was usually less severe than Th1. *Fig. 1* shows the typical electrophysiological findings in a patient with neurogenic TOS. Five patients without clinical neurological deficit were diagnosed as 'non-specific TOS'. In 2 of these patients, subclinical C8-Th1 axon loss was detected by electrophysiological assessment.

Ultrasonography

In one patient (Patient 20) a large bony cervical rib articulating with the first rib was found on the affected, right side. The anterior, articulating end of the cervical rib bulging in the supraclavicular fossa compressed the subclavian artery from the lateral direction and elevated and compressed the lower trunk of the brachial plexus from underneath (*Fig. 2*). The lower trunk was enlarged and hypoechoic. This patient also experienced Raynaud phenomenon in the right arm. On the contralateral side, a smaller, non-articulating cervical rib was present, without any signs of brachial plexus abnormality or compression.

In the remaining 19 patients, in the supraclavicular fossa, slightly cranial to the attachment of the scalene muscles on the 1st rib, the lower trunk of the brachial plexus was indented (compressed

from the lateral direction) by a wedge-shaped, hyperechoic fibromuscular structure at the medial edge of the middle scalene muscle, resulting in a sickle-shaped lower trunk (*Figs. 3-4*). Furthermore, at the site of indentation the lower trunk was markedly hypoechoic, associated with complete loss of fascicular structure, as visually compared to the other trunks of the brachial plexus in the same patient, and also enlarged, as statistically compared to the control group. The mean CSA of the lower trunk, measured at the site of compression, including the whole sickle-shaped structure (i.e. the flattened indented site and the enlarged superficial and deep parts) was 32.6 ± 8.7 mm^2 (range: 20-50 mm^2) in the patient group, and 16.7 ± 3.9 mm^2 (range: 9-23 mm^2) in the control group. The difference between the two groups was statistically significant ($p<0.0001$). In 4 patients, a similar, but less conspicuous wedge-sickle sign was seen also on the unaffected side, and in one patient, the anomalous attachment of the anterior scalene muscle was seen between the subclavian artery and the brachial plexus on the unaffected side. However, in none of the control subjects was a wedge-sickle sign or other anomaly detected. The association between the clinical symptoms and signs suggestive of TOS (including both neurogenic and non-specific TOS) and the presence of the wedge-sickle sign was statistically highly significant ($p<0.0001$). With respect to the clinical signs and symptoms suggestive of TOS (including both neurogenic and non-specific TOS), the presence of the wedge-sickle sign had a sensitivity of 95% (95% CI: 75.13% to 99.87%) and a positive predictive value of 82.6% (95% CI: 61.22% to 95.05%) in our cohort. In addition to the wedge-sickle sign, in Patient 10 the anomalous insertion of the anterior scalene muscle between the subclavian artery and the brachial plexus was also seen (*Fig. 4B*).

In 2 patients (Patients 1 and 5), the fibromuscular structure with the hyperechoic tip indented the subclavian artery as well, caudal to the level of the compression of the lower trunk (*Fig. 5, Supplementary video*). No vascular symptoms were present in these patients. In the patient with the bony articulating cervical rib, the subclavian artery was compressed by the cervical rib. In this patient, Raynaud symptoms were also present indicating vascular involvement.

In 5 patients, the cranial end of the hyperechoic fibromuscular structure was traced to a bony structure with posterior acoustic shadowing (*Supplementary video*). All of these patients had either a cervical rib or an elongated C7 transverse process on the radiography of the cervical spine. In the

remaining patients, cranially the hyperechoic fibromuscular structure gradually melted into the middle scalene muscle.

The attachment of the middle scalene muscle on the first rib is normally found lateral-posterior to the brachial plexus, being the lateral border of the interscalenic space (*Fig. 3A*). In 6 patients, the attachment was more medial-anterior, intruding between the first rib, and the subclavian artery-brachial plexus, and thus elevating the artery and the plexus (*Fig. 6*, *Supplementary video*). This anatomical situation has a space restricting effect in the caudal aspect of the interscalenic space.

Supraclavicular sonographic Tinel sign was observed in 10 patients with the wedge-sickle sign on the affected side, and in the one patient with the articulating cervical rib. In these patients, pressing on the wedge-sickle sign / articulating rib with the transducer provoked strong radiating, electric-like pain and paraesthesia in the arm or the shoulder region. This never occurred in the control subjects, nor in the unaffected arms in the patient group, including those four patients where the wedge-sickle sign was observed in the unaffected arm as well. The association between the presence of the sonographic Tinel sign and the presence of the wedge-sickle sign was statistically highly significant ($p<0.0001$). With respect to the clinical symptoms of neurogenic or non-specific TOS, the presence of a supraclavicular Tinel sign had a sensitivity of 55% (95% CI: 31.53% to 76.94%) and a positive predictive value of 100% (95% CI: 71.51% to 100.00%) in our cohort.

Surgical findings

Eight patients underwent surgery (*Table 1*). The remaining patients either refused surgery or surgery has not been scheduled yet. In Patient 3, the whole middle scalene muscle was found hard and fibrotic and scalenotomy was performed. In Patients 11-14 and 17, at the medial edge of the middle scalene muscle a hard, fibrotic ligament, indenting the lower trunk of the brachial plexus was found. The ligament was resected (*Fig. 7*). The hourglass-like enlargement of the trunk was also observed. In Patient 18, the ligament at the medial edge of the middle scalene muscle was found attached to the elongated transverse process of the 7^{th} cervical vertebra. The ligament was resected. In Patient 24, the ligament at the medial edge of the middle scalene muscle was attached to a cervical rib, but only the

rib was removed. In all patients, pain and paraesthesia in the arm decreased markedly after surgery, as reported by the patients. Long-term follow-up is pending.

DISCUSSION

Our cohort of 20 consecutive patients with TOS shows the clear preponderance of female sex, the early onset of symptoms in youth or middle age, and the preferential involvement of the right (dominant) arm. Fifteen patients were diagnosed with 'neurogenic TOS' indicated by clinical signs of the damage of the lower trunk of the brachial plexus, and 5 fell into the category of 'non-specific TOS', with only subjective symptoms with or without subclinical electrophysiological changes. In one patient with non-specific TOS, a large bony cervical rib articulating with the first rib compressed the brachial plexus (*Fig. 2*). In the remaining 19 patients, a distinctive ultrasonographic sign was observed, which we termed as the '*wedge-sickle sign*' (*Figs 3-4, 8*). The 'wedge' corresponds to a fibromuscular structure with a pointed, hyperechoic (fibrotic) tip along the caudal medial edge of the middle scalene muscle, indenting (compressing) the lower trunk from the lateral direction in the supraclavicular fossa, where it is lodged between the middle scalene muscle and the subclavian artery. The 'sickle' is the shape assumed by the lower trunk in cross-section due to the indentation. The hypoechogenicity, the complete loss of fascicular structure and the significant enlargement of the lower trunk were associated features in all patients, which are characteristic ultrasonographic signs of nerve compression in general (Hobson-Webb et al., 2012). The wedge-sickle sign was also seen in the unaffected arm in four patients, but in none of the control subjects, possibly indicating a genetic predisposition to bilateral occurrence. With respect to the clinical symptoms of neurogenic or non-specific TOS, the wedge-sickle sign had a sensitivity of 95% and a positive predictive value of 82.6% in our cohort. Supraclavicular sonographic Tinel sign was also an important feature, with a lower sensitivity (55%), but with a 100% positive predictive value. The fibromuscular structure may also indent the subclavian artery in the same fashion *(Fig. 5, Supplementary video*), possibly leading to vascular symptoms as well. Moreover, vascular TOS may also cause neurological symptoms secondary to blood vessel involvement, such as pain and numbness of the arm, resembling symptoms

of non-specific TOS. However, in the two patients with the wedge-sickle sign and indentation of the subclavian artery, symptoms were clearly neurological (with marked C8-Th1 axon loss), without associated vascular symptoms. On the other hand, in the one patient with non-specific TOS symptoms where the compression of both the brachial plexus and the subclavian artery was caused by a bony cervical rib, vascular symptoms (Raynaud phenomenon) were also present. It has been shown that the bony cervical rib has a higher relevance for arterial vascular TOS (Weber and Criado, 2014). In this patient, the difference between symptoms of brachial plexus and of arterial origin is not so clearly delineated.

The observed fibromuscular structure located between the lower trunk and the middle scalene muscle in the supraclavicular fossa may correspond to several of the 10 different types of bands causing compression of the Th1 root or the lower trunk described by Roos (1980). In type 1, a tight fibrous band connects the rudimentary cervical rib to the mid portion of the first rib, posterior to the scalene tubercle. In type 2, the band originates on an elongated C7 transverse process. In 5 of our patients with the wedge-sickle sign, the cranial end of the fibromuscular structure could be traced to a bony structure with posterior acoustic shadowing (*Supplementary video)*. As all of these patients had a cervical rib or an elongated C7 transverse process, the bony structure appearing in the interscalenic region cranial to the site of compression most likely corresponds to the anterior tip of the cervical rib or the elongated C7 transverse process. Thus, type 1 or 2 bands are probably the cause of the compression in this subset of patients. In the remaining patients with the fibromuscular abnormality, the wedge shaped fibromuscular structure became less distinct cranially and melted into the middle scalene muscle. In these cases, the other types of Roos ligaments (types 3-10) are considered, but they cannot be reliably differentiated from each other on ultrasound. Type 3 (a fibromuscular band arising at the neck of the first rib and attaching to the inner part of the first rib, posterior to the scalene tubercle) is the most common type according to Roos (1976), and type 4 (fibrous, sharp medial edge of the middle scalene muscle, and medial attachment of the muscle) is also noteworthy. In the latter, the more medial (anterior) attachment of the middle scalene muscle leads to a common tendinous insertion of the anterior and middle scalene muscles, forming a V-shaped sling underneath the subclavian artery and the lower trunk (*Fig. 6*). This anatomical situation elevates the lower trunk from

the first rib and may result in a space occupying effect and compression of the lower trunk, especially if the middle scalene muscle has a sharp, fibrous medial edge. However, we observed this anomalous attachment in patients with type 1 or 2 bands as well, where it may be considered as an additional factor contributing to the compression. Furthermore, in Patient 10 the anomalous insertion of the anterior scalene muscle between the subclavian artery and the brachial plexus was seen, thus in this patient the lower trunk became compressed between the middle and the anterior scalene muscles (*Fig. 4B*).

The presurgical identification of the fibromuscular structure as the cause of compression of the lower trunk is especially important in the controversial 'non-specific TOS' category. In our cohort, the '*wedge-sickle sign*' associated with sonographic Tinel sign could also be demonstrated in 4 patients with only pain and paraesthesia in the arm without neurological deficit (*Fig. 4*). Likewise, in a surgical series of 14 patients, it was shown that anomalous fibromuscular bands compressed the lower trunk in patients with only pain, sensory symptoms and supraclavicular Tinel sign (Liu et al. 1995). Furthermore, in a recent study, the compression of the lower trunk was identified by MRI in three cases of 'non-specific TOS' (Baumer et al. 2014). Thus, it may be necessary to reconsider the validity of the category of 'non-specific TOS'. Patients with only the typical subjective symptoms of TOS, associated with imaging proof of lower trunk compression, should be classified as 'neurogenic TOS', as they just represent an early stage of the disease. This has clinical relevance, as in patients with already marked C8-Th1 axon loss, surgery mainly only stops progression; proximodistal axonal regrowth is unlikely due to the long distance (Ferrante 2012). In a retrospective analysis of the surgical outcome of TOS patients with atrophy, only minimal recovery was observed in close to 50% of the patients (Marty et al. 2012). In view of this, the early identification of TOS patients should be the goal, where imaging modalities such as ultrasound and MRI (Aralasmak et al. 2012; Luigetti et al. 2012; Matur et al. 2013; Yildizgören et al. 2014; Singh et al. 2014; Baumer et al. 2014; Magill et al. 2015; Poretti et al. 2015) may play an important role. Ultrasound is a more easily accessible modality, however MRI may be the appropriate choice in patients with an unfavourable body habitus.

Limitations of our study include the retrospective nature of the analysis and the lack of surgical confirmation of the fibromuscular anomaly in all patients. A further limitation may be that the

examinations were carried out by different ultrasonographers on different ultrasound devices. However, inter-rater and inter-equipment reliability in nerve ultrasound has been tested previously, confirming examiner, and equipment-independent reproducibility (Kluge et al. 2010; Böhm et al. 2014).

SUMMARY

Our study provides ultrasonographic confirmation of Roos' observation that anomalous fibromuscular structures in the scalenic triangle are the major causes of neurogenic TOS. We report a novel and distinctive ultrasonographic sign, the '*wedge-sickle sign*', which allows the easy presurgical identification of these bands causing TOS. This is especially useful in patients without neurological deficit, where the diagnosis is not always as straightforward. On the other hand, early diagnosis is important, because the neurological deficit associated with TOS may be irreversible.

Acknowledgements: Zsuzsanna Arányi and Anita Csillik were supported by the National Brain Research Program (NAP B) of the Hungarian government (KTIA_NAP_13-2-2014-0012). The funding source had no direct role in the design of the study, the interpretation of the data or the preparation / submission of the manuscript.

Financial disclosure / conflicts of interest: None to declare.

References

Aralasmak A, Cevikol C, Karaali K, Senol U, Sharifov R, Kilicarslan R, Alkan A. MRI findings in thoracic outlet syndrome. Skeletal Radiol 2012; 41:1365-1374.

Baumer P, Kele H, Kretschmer T, Koenig R, Pedro M, Bendszus M, Pham M. Thoracic outlet syndrome in 3T MR neurography-fibrous bands causing discernible lesions of the lower brachial plexus. Eur Radiol 2014; 24:756-761.

Böhm J, Scheidl E, Bereczki D, Schelle T, Arányi Z. High resolution ultrasonography of peripheral nerves: measurements on 14 nerve segments in 56 healthy subjects and reliability assessments. Ultraschall Med 2014; 35:459-467.

Brantigan CO, Roos DB. Etiology of neurogenic thoracic outlet syndrome. Hand Clin 2004; 20:17-22.

Ferrante MA. The thoracic outlet syndromes. Muscle Nerve 2012; 45:780-795.

Gilliatt RW, Le Quesne PM, Logue V, Sumner AJ. Wasting of the hand associated with a cervical rib or band. J Neurol Neurosurg Psychiatry 1970; 33:615-624.

Gruber H, Glodny B, Galiano K, Kamelger F, Bodner G, Hussl H, Peer S. High-resolution ultrasound of the supraclavicular brachial plexus— Can it improve therapeutic decisions in patients with plexus trauma? Eur Radiol 2007; 17:1611–1620.

Hobson-Webb LD, Padua L, Martinoli C. Ultrasonography in the diagnosis of peripheral nerve disease. Expert Opin Med Diagn 2012; 6:457-471.

Kluge S, Kreutziger J, Hennecke B et al. Inter- and intraobserver reliability of predefined diagnostic levels in high-resolution sonography of the carpal tunnel syndrome – a validation study on healthy volunteers. Ultraschall in Med 2010; 31: 43–47.

Liu JE, Tahmoush AJ, Roos DB, Schwartzman RJ. Shoulder-arm pain from cervical bands and scalene muscle anomalies. J Neurol Sci 1995; 128:175-180.

Luigetti M, Capone F, Di Lazzaro V. Teaching neuroimages: neurogenic thoracic outlet syndrome. Neurology 2012; 79:e11.

Magill ST, Brus-Ramer M, Weinstein PR, Chin CT, Jacques L. Neurogenic thoracic outlet syndrome: current diagnostic criteria and advances in MRI diagnostics. Neurosurg Focus 2015; 39:E7.

Martinoli C, Bianchi S, Santacroce E, Pugliese F, Graif M, Derchi LE. Brachial plexus sonography: A technique for assessing the root level. AJR Am J Roentgenol 2002; 179:699–702.

Marty FL, Corcia P, Alexandre J, Laulan J. True neurological thoracic outlet syndrome. Retrospective study of 30 consecutive cases. Chir Main 2012; 31:244-259.

Matur Z, Dikici F, Salmaslioglu A, Sencer S, Baslo B, Oge E. Teaching neuroimages: swollen T1 nerve root in neurogenic thoracic outlet syndrome. Neurology 2013; 80:e247.

Peete RM, Heriksen MD, Anderson TP. Thoracic outlet syndrome: evaluation of a therapeutic exercise program. Mayo Clin Proc 1956; 31:281–287.

Plewa MC, Delinger M. The false-positive rate of thoracic outlet syndrome shoulder maneuvers in normal subjects. Acad Emerg Med 1998; 5:337–342.

Poretti D, Lanza E, Sconfienza LM, Mauri G, Pedicini V, Balzarini L, Sardanelli F. Simultaneous bilateral magnetic resonance angiography to evaluate thoracic outlet syndrome. Radiol Med 2015; 120:407-412.

Roos DB. Congenital anomalies associated with thoracic outlet syndrome. Anatomy, symptoms, diagnosis, and treatment. Am J Surg 1976; 132:771–778.

Roos DB. Pathophysiology of congenital anomalies in thoracic outlet syndrome. Acta Chir Belg 1980; 79:353-361.

Simon NG, Ralph JW, Chin C, Kliot M. Sonographic diagnosis of true neurogenic thoracic outlet syndrome. Neurology 2013; 81:1965.

Singh VK, Jeyaseelan L, Kyriacou S, Ghosh S, Sinisi M, Fox M. Diagnostic value of magnetic resonance imaging in thoracic outlet syndrome. J Orthop Surg (Hong Kong) 2014; 22:228-231.

Tsao BE, Ferrante MA, Wilbourn AJ, Shields RW. Electrodiagnostic features of true neurogenic thoracic outlet syndrome. Muscle Nerve 2014; 49:724-727.

Viertel VG, Intrapiromkul J, Maluf F, Patel NV, Zheng W, Alluwaimi F, Walden MJ, Belzberg A, Yousem DM. Cervical ribs: a common variant overlooked in CT imaging. AJNR Am J Neuroradiol 2012; 33:2191-2194.

Weber AE, Criado E. Relevance of bone anomalies in patients with thoracic outlet syndrome. Ann Vasc Surg 2014; 28:924-932.

Wilbourn AJ. Thoracic outlet syndromes. Neurol Clin 1999; 17:477-497.

Yildizgören MT, Ekiz T, Kara M, Yörübulut M, Ozçakar L. Magnetic resonance imaging of a fibrous band causing true neurogenic thoracic outlet syndrome. Am J Phys Med Rehabil 2014; 93:732-733.

Figure legends

Figure 1

Typical electrophysiological findings in neurogenic TOS

Motor and sensory nerve conduction studies in a patient with neurogenic TOS on the left side (Patient 6). Note the low amplitude motor and sensory responses in C8-Th1 distribution, the innervation area of the lower trunk of the brachial plexus on the left side, as compared with the unaffected right side. Note also that the amplitude reduction in Th1 supplied areas (thenar muscle-median nerve motor response, MABC sensory response) is greater than that in C8 supplied areas (ulnar nerve motor and sensory responses). Amplitude reduction indicates axon loss. All side comparisons are shown with the same gain and sweep settings.

NCS: nerve conduction studies; R: right; L: left; MABC: medial antebrachii cutaneous nerve; NR: no response

Figure 2

Cervical rib compressing the brachial plexus

Axial image of the supraclavicular brachial plexus of Patient 20, showing the bony anterior end of a large cervical rib articulating with the first rib and bulging into the supraclavicular fossa (arrow). Note how it elevates and compresses the lower trunk, the medial part of the brachial plexus (dotted line) and compresses the subclavian artery (dashed line) from the lateral direction. The lower trunk is hypoechoic.

Med: medial; Lat: lateral; AS: anterior scalene muscle; Art: subclavian artery;

Figure 3

Spectrum of the ‘wedge-sickle’ sign

Axial images show the lower trunk (dotted line) in the supraclavicular fossa (**A**: Normal control, **B**: Patient 4, .**C**: Patient 5, **D**: Patient 1, **E**: Patient 6, **F**: Patient 12). Note the hyperechoic pointed fibromuscular structure at the caudal medial aspect of the middle scalene muscle indenting the lower trunk adjacent to the subclavian artery.

Med: medial; Lat: lateral; AS: anterior scalene muscle; MS: middle scalene muscle; Art: subclavian artery; asterisk (*): hyperechoic tip of the fibromuscular structure

Figure 4

The 'wedge-sickle' sign in patients without neurological deficit

A and **B** show the 'wedge-sickle' sign in patients without neurological deficit (Patients 9 and 10, respectively). The dotted line outlines the lower trunk. Note also the anomalous insertion of the anterior scalene muscle in **B**.

Med: medial; Lat: lateral; AS: anterior scalene muscle; MS: middle scalene muscle; Art: subclavian artery; asterisk (*): hyperechoic tip of the fibromuscular structure

Figure 5

Indentation of the subclavian artery

A and **B** show the fibromuscular structure indenting the subclavian artery (Patient 5, caudal to the image in Fig. 3C) with and without colour Doppler, respectively. The lower trunk is round at this level (dotted line).

Med: medial; Lat: lateral; AS: anterior scalene muscle; MS: middle scalene muscle; Art: subclavian artery; asterisk (*): hyperechoic tip of the fibromuscular structure

Figure 6

Anomalous attachment of the middle scalene muscle

Axial images in the most caudal aspect of the supraclavicular fossa of Patient 1 (**A**) and 5 (**B**). Note the unusually medial (anterior) attachment of the middle scalene muscle (outlined by dotted line), elevating the subclavian artery and the brachial plexus from the 1st rib.

Med: medial; Lat: lateral; AS: anterior scalene muscle; MS: middle scalene muscle; Art: subclavian artery; asterisk (*): hyperechoic tip of the fibromuscular structure

Figure 7

Intraoperative confirmation of the 'wedge-sickle sign'

A. Axial ultrasonographic image of Patient 17, showing the 'wedge-sickle sign' (the lower trunk outlined by dotted line). **B-D** show successive intraoperative steps. Note the swollen lower trunk and the indentation on the trunk, visible after resection of the ligament (**D**).

Med: medial; Lat: lateral; AS: anterior scalene muscle; MS: middle scalene muscle; Art: subclavian artery; asterisk (*): hyperechoic tip of the fibromuscular structure

Figure 8

Schematic representation of the 'wedge-sickle' sign

LT: lower trunk; Art: subclavian artery; asterisk (*): hyperechoic tip of the fibromuscular structure

Table 1. Summary of patient characteristics and findings

Case No.	Age (year)	Duration (year)	Side (L/R)	Neurological deficit	Pain	EDX (C8-Th1 axon loss)	CSA of the lower trunk (mm^2)	Radiography (cervical rib / elongated C7)	Surgery
1	64	16	R	Th1 > C8	-	Th1 > C8	29	C7	-
2	27	1	L	Th1 > C8	-	Th1 > C8	47	-	-
3	38	1	L	Th1 > C8	+	Th1 > C8	40	Rib	+
4	36	<1	R	Th1 > C8	+	Th1 > C8	40	-	-
5	37	3	R	Th1 > C8	-	Th1 > C8	20	Rib	-
6	28	5	L	Th1 > C8	-	Th1 > C8	50	Rib	-
7	27	3	R	-	+	Th1 (sens)	45	-	-
8	46	10	R	-	+	-	20	Rib	-
9	40	2	R	-	+	C8-Th1 (sens)	25	C7	-
10	19	2	R	-	+	-	22	-	-
11	74	5	R	Th1 > C8	-	Th1 > C8	29	-	+
12	43	2	R	Th1 > C8	+	Th1 > C8	34	-	+
13	54	5	R	Th1 > C8	+	Th1 > C8	30	Rib	+
14	49	15	R	Th1 > C8	+	Th1 > C8	36	C7	+
15	53	3	R	Th1 - C8	+	C8-Th1	34	-	-
16	43	2	R	Th1 > C8	+	Th1 > C8	22	-	-
17	57	13	R	C8-Th1	-	C8-Th1	30	C7	+
18	21	2	R	C8-Th1	-	C8-Th1	37	C7	+
19	24	2	R	C8-Th1	+	C8-Th1	32	Rib	+
20	28	14	R	-	+	-	30	Rib	-

L: left; R: right; CSA: cross-sectional area; sens: only sensory; EDX: electrophysiological examination

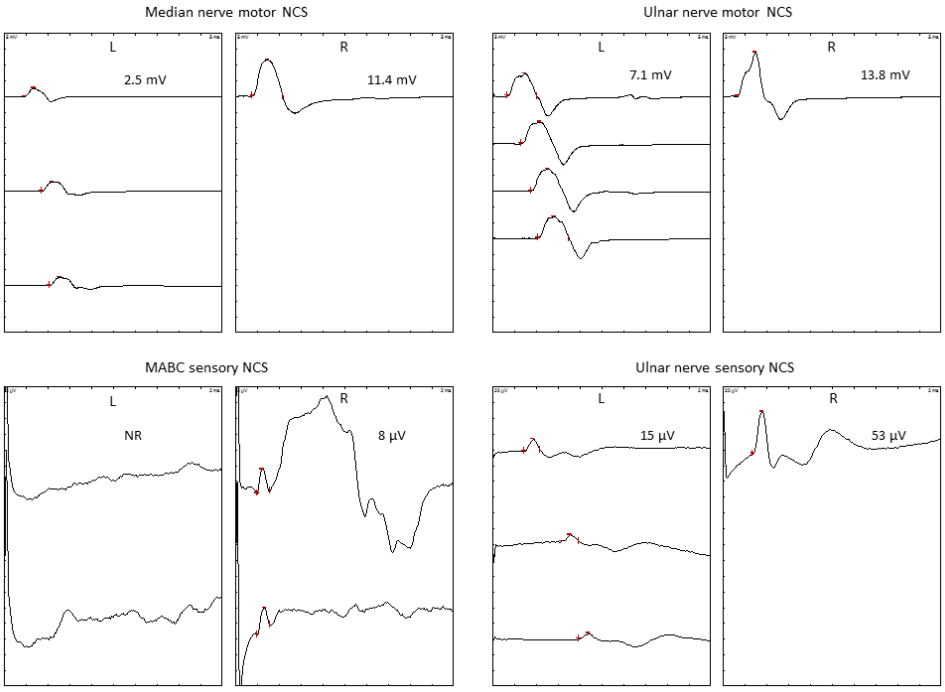
Median nerve motor NCS
L
2.5 mV
R
11.4 mV
Ulnar nerve motor NCS
L
7.1 mV
R
13.8 mV
MABC sensory NCS
L
NR
R
8 µV
Ulnar nerve sensory NCS
L
15 µV
R
53 µV

Fig. 1

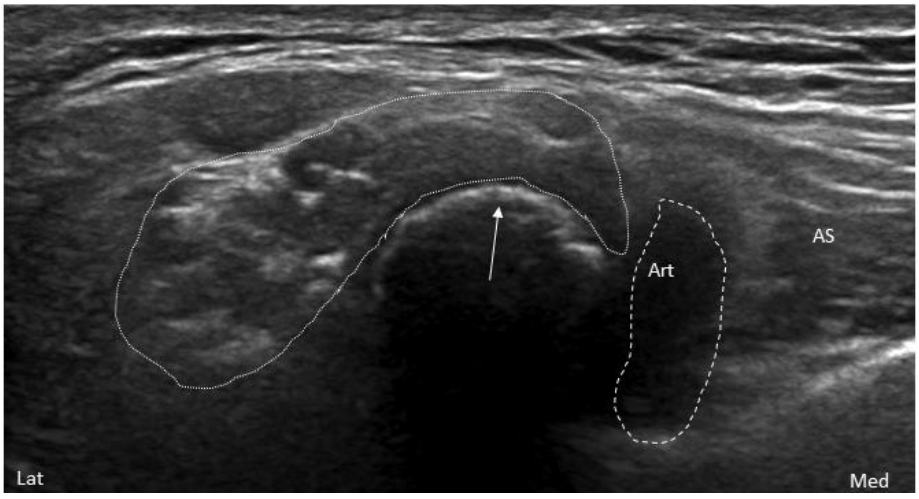
AS
Art
Lat
Med

Fig. 2

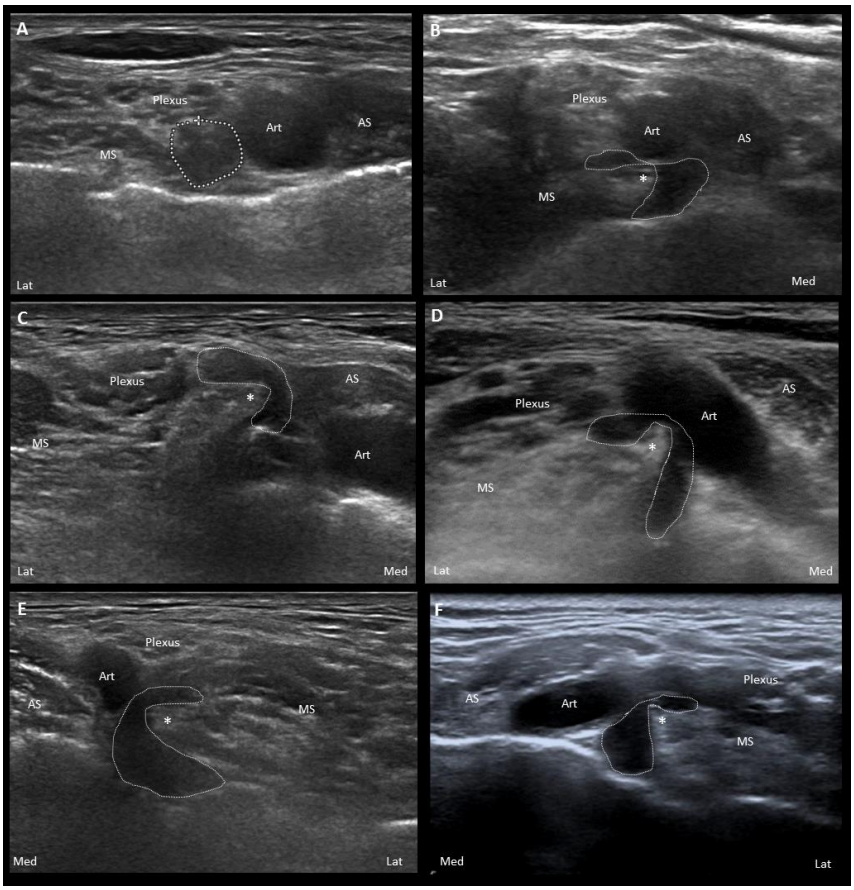

Fig. 3

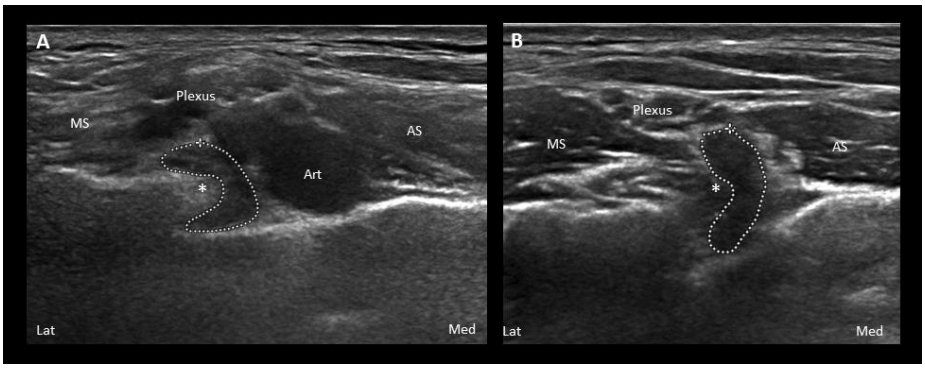

Fig. 4

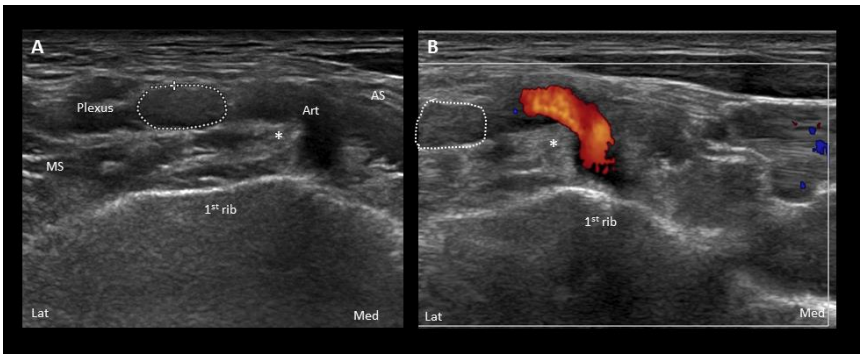

Fig. 5

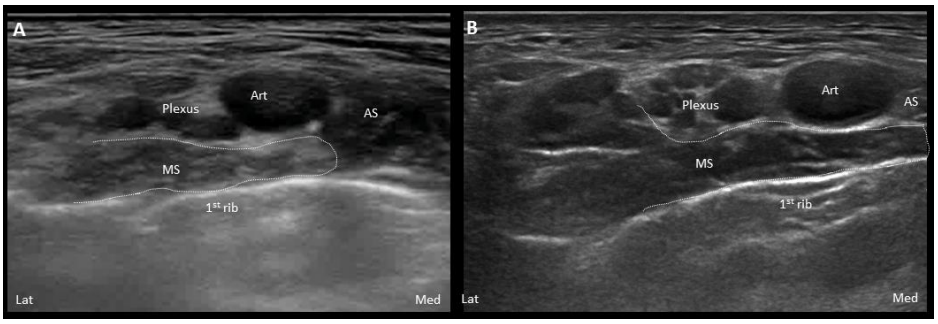

Fig. 6

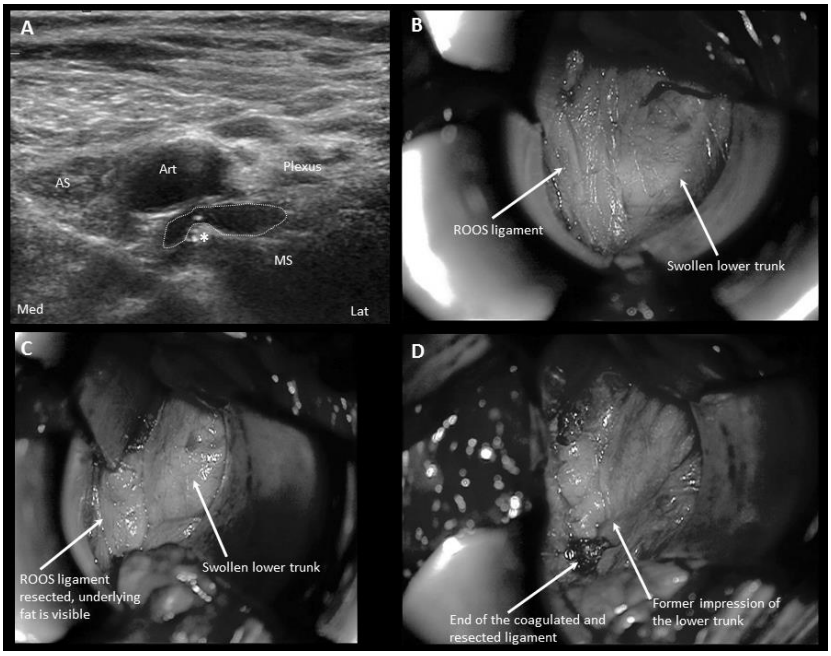

Fig. 7

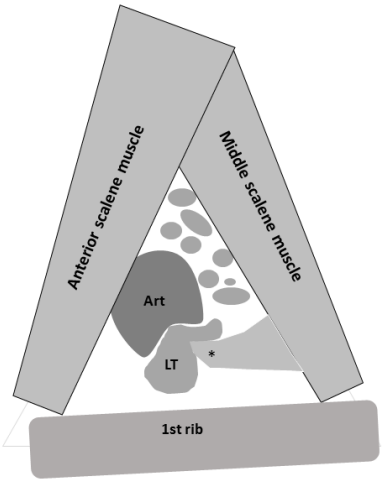

Fig. 8